

RESEARCH ARTICLE

Design Principles for Maximization of an Inductive Power Transfer System Inherent Tolerance to the Coils Misalignment

EDUARD MINDUBAEV¹, (Member, IEEE), KONSTANTIN GUROV¹, (Member, IEEE),
SERGEY SELISHCHEV¹, (Senior Member, IEEE), AND ARSENY DANILOV¹, (Member, IEEE)

Institute of Biomedical Systems, National Research University of Electronic Technology (MIET), Zelenograd, 124482 Moscow, Russia

Corresponding author: Eduard Mindubaev (edmindubaev@gmail.com)

This work was supported by the State Assignment given by the Ministry of Science and Higher Education of the Russian Federation, in December 2019, under Agreement 075-03-2020-216.

ABSTRACT This paper presents an analysis of the inductive power transfer system (IPT) in terms of its tolerance to the coils misalignment. We introduce two new metrics, which we refer to as misalignment tolerance (MT) and α , for formal assessment of the IPT system tolerance to the misalignment. Using these metrics, we evaluate two common design scenarios: an IPT system with maximized power transfer efficiency (PTE) and an IPT system with maximized power delivered to the load (PDL). Based on this analysis, we formulate design principles aimed at maximizing the inherent tolerance of the IPT system to the coils misalignment, i.e. the tolerance that is achieved before adding control loops in the IPT system. The presented principles cover both the system level, where the coils geometry is fixed, and the coil couple level, where the coils geometry is optimized. We derive an analytical equation for the calculation of the optimal critical coupling, which leads to the maximization of MT. We also present an exemplary coils optimization procedure for the improvement of MT. The procedure demonstrates that an IPT system with an asymmetrical number of turns achieves higher MT. To validate our findings, four IPT system prototypes with different values of critical coupling, as well as optimized and non-optimized coils were manufactured and compared. The IPT systems with non-optimized and optimized coils exhibited MT of 73% and 82%, correspondingly.

INDEX TERMS Coils displacement, coils misalignment, critical coupling, inductive power transfer, wireless power transfer.

I. INTRODUCTION

Inductive power transfer (IPT) is a rapidly evolving technology that finds applications in different fields, such as implantable medical electronics, consumer electronics, electric vehicles charging and more [1], [2], [3], [4], [5], [6]. While IPT systems can provide highly efficient non-contact power transfer, there are still some design problems that need to be addressed and some aspects of these systems that can be improved [7], [8], [9]. One of the main problems of IPT systems is coils misalignment. Displacements of the coils from their optimal relative position can result in the

reduced efficiency of the IPT system as well as insufficient or excessive output power and, therefore, potential device failure.

Main approaches for addressing the misalignment problem are: mechanical fixation of the relative coil position; circuit enhancement, i.e. use of feedback loops and control schemes; optimization of the geometric parameters of the coils. Mechanical fixation of the relative coil position can solve the problem of misalignments, but it is not a universal solution and its application is limited to niche cases [10], [11]. The application of feedback loops and control schemes enables the design of IPT systems with high tolerance to misalignments [12], [13], [14], [15], [16], [17]. This approach is more versatile and can be used in many different

The associate editor coordinating the review of this manuscript and approving it for publication was Xiaodong Liang¹.

applications. However, it has some drawbacks, such as: additional power requirements, reduced overall efficiency of the system and increased design complexity, which lowers the system reliability. Overall, despite numerous proposed specialized schemes that can mitigate the impact of the coils misalignment within certain frequency, power, and system size ranges, the misalignment problem cannot be considered fully solved.

This article focuses on the last one of the mentioned approaches, i.e. the optimization of the geometric parameters of the coils [18], [19], [20], [21], [22], [23], [24]. Scientific articles dedicated to the issue of the coils misalignment are numerous. However, typical results presented in these articles usually are either specific geometry of inductive coils or an algorithm for designing inductive coils. Usually, the articles demonstrate the dependencies of system characteristics (such as output voltage, output power, efficiency, gain coefficient) on coupling coefficient, mutual inductance, or specific type of the misalignment (axial, lateral, etc.). The presented dependencies provide insights into the characteristics of a specific IPT system and can be used for improving the tolerance to the misalignment. However, applying the results from these articles to IPT systems with different design parameters can be a challenging task. In other words, the drawback of the existing articles is the lack of general design principles that enable the inherent tolerance to the coils misalignment.

The main goal of this paper is the identification of such principles. Systematic framework is presented for the design and optimization of an IPT system operating in the presence of the coils misalignment. Two common approaches to an IPT system optimization, i.e. maximization of PDL and PTE, are considered in the paper. The proposed framework should be useful as an additional design consideration for aiding in resolving the tradeoff between PDL and PTE by introducing new parameter characterizing the IPT system, the misalignment tolerance (MT).

Previously, the algorithm to minimize the drop in PDL in a given range of the coils misalignment was designed [20]. However, in this algorithm the resulting PDL drop could not be estimated before the procedure finish, therefore this approach lacked predictive power. One of the contributions of the current paper is that we can relate changes in geometrical parameters with changes in PDL and PTE analytically, and, therefore, design new optimization procedures upon that. Examples of such procedures are presented in the paper.

Key contributions provided by this paper can be shortly summarized as follows:

1. We have shown how the relative change in PDL and PTE resulting from the coils misalignment is influenced by a relation of the coupling coefficient and the critical coupling, and a relation of the maximum to minimum coupling coefficient in a given range of the coils misalignment.

2. We have shown that the theoretical limit of the misalignment tolerance for a given coil couple and preset

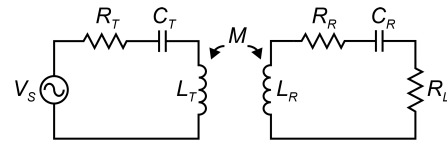


FIGURE 1. An inductive power transfer system with series-series compensation.

values of expected (possible) misalignment is achieved via tuning to the critical coupling coefficient equal to the square root of product of the minimum and maximum coupling coefficients in the expected range of the coils misalignment.

3. We introduced two new metrics to formally assess an IPT system misalignment tolerance. The first one, which we refer to as MT, is defined as the ratio of minimum to maximum PDL in the given range of the coils misalignment. The second metric is denoted as α and is defined as the square root of the ratio of minimum to maximum coupling coefficient.

4. We presented the comparison between the IPT systems optimized for maximum PDL and maximum PTE in terms of their tolerance to the coils misalignment with the help of the newly introduced metrics, namely, MT and α . We have shown that the tolerance to the coils misalignment is solely influenced by α .

The paper is structured as follows: Section II demonstrates a conventional approach for the evaluation of an inductive link behavior based on circuit analysis. In Section III we introduce a framework for the estimation of an IPT system tolerance to the coils misalignment and the new metric, i.e. MT. We estimate MT for two optimization scenarios of an IPT system: an IPT system with maximized PDL and an IPT system with maximized PTE. In Section IV we describe an exemplary coils optimization procedure and considerations for the design of the IPT system. In Section V we provide an experimental verification of the presented concepts. Finally, in the Conclusion we summarize the design principles aimed at the maximization of the IPT system tolerance to the coils misalignment.

II. DESCRIPTION OF THE IPT SYSTEM

Fig. 1 shows an IPT system with series-series compensation. The circuit is supplied by a voltage source V_S . L_T and L_R are transmitting and receiving coils, C_T and C_R are compensating capacitors. The transmitter and receiver are tuned to the resonant frequency ω_{res} :

$$\omega_{res} = \frac{1}{\sqrt{L_T C_T}} = \frac{1}{\sqrt{L_R C_R}} \quad (1)$$

The equivalent resistance of the transmitter R_T is a sum of the equivalent series resistance (ESR) of the transmitting coil and other resistances in the circuit. The equivalent resistance of the receiver of the IPT system R_R is the ESR of the receiving coil. R_L is the equivalent load of the IPT system. M is the mutual inductance between the coils. Coupling coefficient k is a fraction of magnetic flux generated by one

coil that crosses the other coil:

$$k = \frac{M}{\sqrt{L_T L_R}} \quad (2)$$

The quality factor of the transmitter Q_T and the loaded quality factor of the receiver Q_R can be calculated as:

$$Q_T = \frac{1}{R_T} \sqrt{\frac{L_T}{C_T}} \quad (3)$$

$$Q_R = \frac{1}{R_R + R_L} \sqrt{\frac{L_R}{C_R}} \quad (4)$$

The absolute value of PDL can be found by applying Kirchhoff's laws to the circuit shown in Fig. 1:

$$P_L = \frac{\omega^2 M^2 V_S^2 R_L}{(R_T(R_R + R_L) + \omega^2 M^2)^2} \quad (5)$$

PTE of the system is defined as follows:

$$\eta = \frac{P_L}{P_S} \quad (6)$$

here, P_S is the total power consumption of the system:

$$P_S = \frac{V_S^2}{Z_{total}} \quad (7)$$

here, Z_{total} is the total impedance of the IPT system. By applying Kirchhoff's laws PTE can be found as:

$$\eta = \frac{\omega^2 M^2 R_L}{(R_R + R_L)(R_T(R_R + R_L) + \omega^2 M^2)} \quad (8)$$

We propose and use alternative forms for the expressions defining key performance metrics of the IPT system, i.e. PDL and PTE. In the proposed representation PDL and PTE are defined through coupling coefficient k and critical coupling k_{crit} . The critical coupling historically attracts an interest of the researchers, because it provides means for the optimization of IPT systems [25], [26]. The critical coupling corresponds to the maximum PDL in a given range of coupling coefficient:

$$\left. \frac{dP_L}{dk} \right|_{k=k_{crit}} = 0 \quad (9)$$

The critical coupling can be found by substituting (2) and (5) into (9), then solving the resulting equation and subsequently substituting (3) and (4) into the solution:

$$k_{crit} = \frac{1}{\sqrt{Q_T Q_R}} \quad (10)$$

The alternative expression for the PDL can be found by using (2), (3), (4) and (10) to rewrite (5):

$$P_L = P_L(k_{crit}) \left(\frac{2k/k_{crit}}{1 + (k/k_{crit})^2} \right)^2 \quad (11)$$

here, $P_L(k_{crit})$ is the PDL at the critical coupling. It can be found by substituting (10) into (2) to find the mutual

TABLE 1. Parameters of IPT systems for different applications: an electric vehicle, a medical implant, a mobile device. Parameters of the systems are similar to [25].

	Electric vehicle	Implantable medical device	Mobile device
Transmitting coil parameters			
Outer radius (mm)	250	12.5	30
Wire radius (mm)	10	0.5	0.8
Pitch (mm)	0.1	0.1	0.1
Number of turns	4	9	2
Self-inductance L_T (μ H)	10.36	1.12	0.48
ESR R_{coilT} (Ω)	0.05	1.71	0.10
Receiving coil parameters			
Outer radius (mm)	225	11	20
Wire radius (mm)	10	0.5	0.3
Pitch (mm)	0.1	0.1	0.1
Number of turns	4	8	4
Self-inductance L_R (μ H)	8.72	0.77	1.25
ESR R_{coilR} (Ω)	0.04	1.26	0.52
IPT system electrical parameters			
Voltage source V_S (V)	100	1.5	5
Source resistance R_S (Ω)	0.5	0.5	0.5
Operating frequency f (kHz)	145	13560	13560
Capacitance C_T (nF)	11.6	0.12	0.29
Capacitance C_R (nF)	13.8	0.18	0.11
Load resistance L_R (Ω)	20	50	10

inductance corresponding to the critical coupling, and then using it to solve (5), resulting in:

$$P_L(k_{crit}) = \frac{V_S^2 R_L}{4R_T(R_R + R_L)} \quad (12)$$

$P_L(k_{crit})$ represents the maximum PDL that can be achieved for given parameters of the IPT system with series-series compensated inductive link. The value of the maximum PDL is a function of solely the source voltage and the resistances in the system. It is not directly affected by other parameters of the IPT system, such as self-inductances of the coils and compensating capacitances. The only parameters of the coils that have effect on the absolute value of the PDL at the critical coupling are their ESR. Therefore, one can knowingly estimate the limit of PDL for given parameters of the IPT system at an early stage of the design.

The other term in (11), namely the bracketed expression, is a dimensionless ratio that describes the effect of the coils misalignment on PDL. It shows that the tolerance of the IPT system to the coils misalignment is a function of the single parameter: k/k_{crit} , that is a rewrite of the figure-of-merit kQ . This rewrite emphasizes the way of thinking about the IPT system operating point in terms of its proximity to the critical coupling. Fig. 2a depicts PDL normalized by the PDL at the critical coupling as a function of k/k_{crit} . This function is a template representing PDL tolerance to the coils misalignment and will hereinafter be referred to as the characteristic form of PDL.

The characteristic form of PDL implies that one can predict analytically a change in PDL as a result of the coils misalignment expressed through the coupling coefficient. For

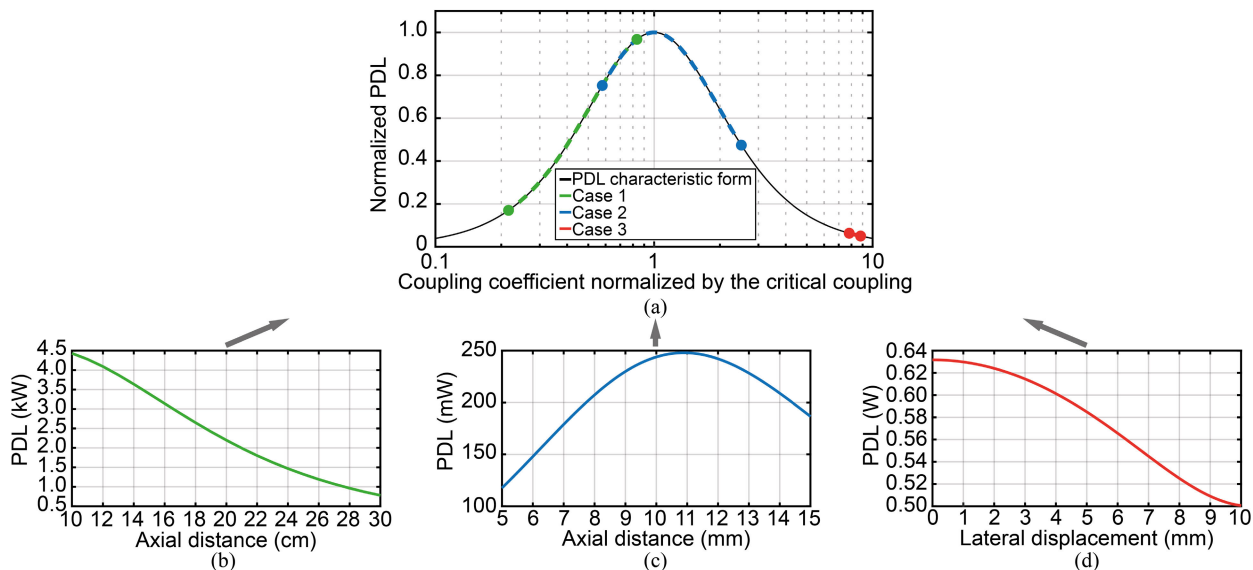


FIGURE 2. The characteristic form of PDL, i.e. PDL of an IPT system normalized by the PDL at the critical coupling as a function of the coupling coefficient normalized by the critical coupling, (a) with PDL as a function of the coils misalignments for IPT systems for different applications, i.e. an electric vehicle (b), an implantable medical device (c) and a mobile device (d), delineated on it. Parameters of the IPT systems are given in Table 1.

example, independently of the absolute values of the coupling coefficient and the critical coupling, PDL is reduced to 64% of its maximum possible value for twofold increase ($k = 2k_{crit}$) or decrease ($k = 0.5k_{crit}$) in the coupling coefficient in relation to the critical coupling. This concept can serve as a basis for optimization procedures of IPT systems with series-series compensation.

To better illustrate the idea behind the characteristic form of PDL, three IPT systems were modeled. Each of these systems corresponds to a specific application of IPT, i.e. an electrical vehicle, an implantable medical device (retinal implant in this case) and a mobile device. The parameters of these IPT systems are given in Table 1 and are similar to examples from the literature [25]. The systems operate in different ranges and types of the coils misalignment. Figs. 2b–2d depict PDL of these systems as a function of the coils misalignment. The IPT system for an electric vehicle operates in range of axial distance between the coils 10... 30 cm (Fig. 2b). The IPT system for an implantable medical device operates in range of axial distance 5... 15 mm (Fig. 2c). The IPT system for a mobile device operates at fixed axial distance 2 mm and in range of lateral misalignment of the coils 0... 20 mm (Fig. 2d). Fig. 2a shows PDL of these three systems delineated on the characteristic form of PDL.

A similar analysis can be done for PTE of the IPT system. The alternative expression form for PTE can be found using (2), (3), (4) and (10) to rewrite (8):

$$\eta = \eta(k_{crit}) \frac{2(k/k_{crit})^2}{1 + (k/k_{crit})^2} \quad (13)$$

here, $\eta(k_{crit})$ is the PTE at the critical coupling. It can be found by solving (8) for the critical coupling condition:

$$\eta(k_{crit}) = \frac{R_L}{2(R_R + R_L)} \quad (14)$$

Unlike in the case of PDL, the PTE at the critical coupling is not equal to its maximum for given parameters of the IPT system. It is limited to 50% and can be even lower, if the ESR of the receiving coil is greater than the load resistance of the IPT system. Throughout the rest of the paper, the load resistance is assumed to be much greater than the ESR of the receiving coil ($R_L \gg R_R$).

The remaining term in (13) is a dimensionless ratio that describes the effect of the coils misalignment on PTE. Fig. 3 depicts PTE as a function of coupling coefficient normalized by the critical coupling. This is the characteristic form of PTE that can be used to predict how PTE of the IPT system will change as a result of the coils misalignment expressed through coupling coefficient. PTE changes monotonically with coupling coefficient, i.e. an increase in coupling coefficient leads to an increase in PTE.

The IPT system cannot have high PDL and high PTE simultaneously. PTE of the IPT system increases with an increase in coupling coefficient, while PDL has a local maximum at the critical coupling. Fig. 4 depicts the tradeoff between PDL and PTE. It can be argued that PDL can be regulated by adjusting the source voltage of the system and, hence, PTE is the most important performance metric of the IPT system. However, increase in the power supply will lead to the increased voltage stress on the transistor switches in the power amplifier, therefore, it cannot be considered as unconditionally optimal solution. Therefore, additional considerations should be taken into account while designing an IPT system.

III. TOLERANCE TO THE COILS MISALIGNMENT

The characteristic forms of PDL and PTE can be used to estimate the tolerance of an IPT system to the coils

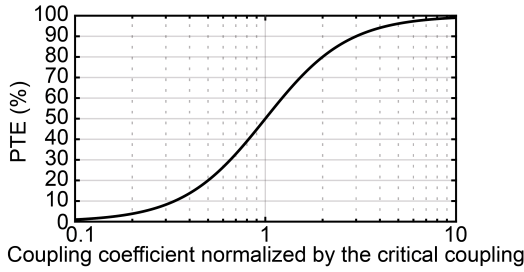


FIGURE 3. PTE of the IPT system as a function of the coupling coefficient normalized by the critical coupling.

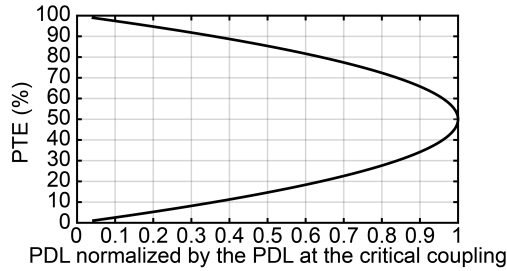


FIGURE 4. Figure-of-merit depicting the tradeoff between PDL of the IPT system normalized by the PDL at the critical coupling and PTE of the IPT system.

misalignment. Two common designs were compared, i.e. an IPT system designed for high and stable PDL and an IPT system designed for high PTE. Both systems operate in the same range of the coils misalignment expressed in terms of coupling coefficient $k_{min} \dots k_{max}$. Here, k_{min} and k_{max} are the lowest and highest coupling coefficient in a given range of the misalignment.

A. IPT SYSTEM WITH MAXIMIZED PDL

For the IPT system shown in Fig. 1 high tolerance to the coils misalignment (in other words, minimal drop in PDL, i.e. $min(P_L|_{k_{min}}^{k_{max}})$) is observed in the vicinity of the critical coupling. However, there are no procedure in the literature that guarantees that the IPT system will be having the highest tolerance to the coils misalignment for a given range of the coils relative positions. As a first step leading to the formulation of such a procedure, we describe the properties of such a system.

We postulate and hereafter prove that the highest tolerance to the coils misalignment in a given range is observed, when values of the PDL at the lowest and highest coupling coefficient are equal. The optimal value of the critical coupling that corresponds to the IPT system with the highest tolerance to the coils misalignment should be equal to k_{stable} :

$$k_{stable} = \sqrt{k_{min}k_{max}} \tag{15}$$

To show that an IPT system with $k_{crit} = k_{stable}$ have the highest tolerance to the coils misalignment. We use the graphical proof depicted in Fig. 5. In this proof we compare PDL for three distinct cases: IPT systems with the critical coupling equal to the optimal coupling k_{stable} ; critical coupling lower than optimal coupling (equal to $0.5k_{stable}$);

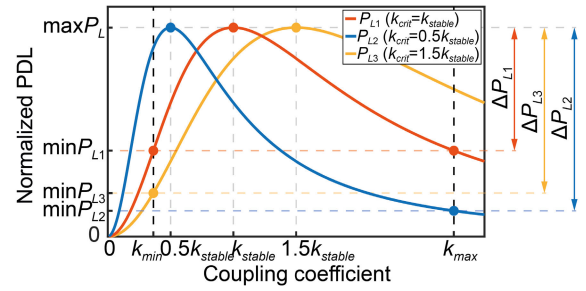


FIGURE 5. PDL normalized by its maximum as a function of coupling coefficient for IPT systems with different values of critical coupling. This figure serves as a graphical proof depicting the optimal critical coupling for a given range of the coils misalignment $k_{min} \dots k_{max}$. The optimal critical coupling provides highest tolerance to the coils misalignment for given coils.

and critical coupling higher than optimal coupling (equal to $1.5k_{stable}$). All three systems operate in the same range of the coils misalignment from k_{min} to k_{max} . Maximum PDL is equal in these systems. The critical coupling in the second system has lower value than in the first one ($k_{crit} = 0.5k_{stable}$). As we can see in Fig. 5, the difference between the maximum and minimum values of PDL in the second system, i.e. $\Delta P_{L2} = max(P_L) - min(P_{L2})$, is greater than the same difference in the first system, i.e. $\Delta P_{L1} = max(P_L) - min(P_{L1})$.

The critical coupling in the third system ($k_{crit} = 1.5k_{stable}$) has higher value than that in the first one. However, in this system the difference between the maximum and minimum values of the PDL, i.e. $\Delta P_{L3} = max(P_L) - min(P_{L3})$, is also greater than in the first system. Therefore, the most stable operation of an IPT system operating in the vicinity of the critical coupling is observed, when the PDL at the lowest possible coupling is equal to the PDL at the highest possible coupling.

Now, when the optimal critical coupling is known, the tolerance of an IPT system to the coils misalignment can be analyzed. To formalize the procedure, an additional performance metric, misalignment tolerance (MT), is introduced. MT is defined as the ratio of the minimum PDL to the maximum PDL in a given range of coils relative positions:

$$MT = \frac{min(P_L)}{max(P_L)} \tag{16}$$

Therefore, low MT equates significant changes in PDL for a given range of the coils misalignment.

For an IPT system operating in the vicinity of the critical coupling, the maximum PDL is observed at the critical coupling. At the same time, if the system is tuned as described above, the minimum PDL will be observed at the lowest and highest coupling. Therefore, (16) can be rewritten as:

$$MT = \frac{P_L(k_{min})}{P_L(k_{crit})} = \frac{P_L(k_{max})}{P_L(k_{crit})} \tag{17}$$

By solving (11) for either lowest or highest coupling coefficient, then substituting the resulting solution into (17),

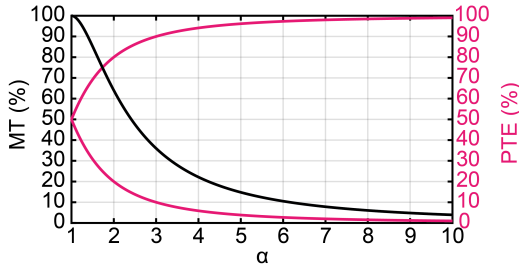


FIGURE 6. MT and PTE of an IPT system operating in the vicinity of the critical coupling as a function of α . Two lines of PTE are boundaries corresponding to the minimum and maximum PTE in a given range of coupling coefficient $k_{min} \dots k_{max}$. Higher α corresponds to a wider range of coupling coefficient and, thus, a wider spread in PTE.

the following expression for MT can be derived:

$$MT = \left(\frac{2\sqrt{k_{min}k_{max}}}{k_{min} + k_{max}} \right)^2 \quad (18)$$

The square root of the ratio of the highest possible coupling coefficient to the lowest one can be denoted as:

$$\alpha = \sqrt{\frac{k_{max}}{k_{min}}} \quad (19)$$

By using (19), (18) can be represented as a function of α :

$$MT = \left(\frac{2\alpha}{\alpha^2 + 1} \right)^2 \quad (20)$$

In its turn, α is defined by the range of the coils misalignment expressed in terms of coupling coefficient. In other words, α is a function of magnetic properties of the coil couple and is not affected by an IPT system electric properties.

From the abovementioned it can be concluded, that MT is also a function of magnetic properties of the coil couple only. Therefore, the main factor limiting tolerance of an IPT system to the coils misalignment is properly optimized geometry of the coils. Fig. 6 depicts MT of an IPT system operating in the vicinity of the critical coupling as a function of α .

An additional implication here is the fact that MT of an IPT system can be estimated, while bypassing a notable part of the system design, e.g. tuning of the capacitors in the transmitter and the receiver, calculation of the optimal critical coupling. Overall, (20) allows to estimate a theoretical limit of MT for an IPT system with specified magnetic properties.

In a similar manner, PTE of an IPT system operating in the vicinity of the critical coupling as a function of α can be found (Fig. 6). Unlike in the case of PDL, boundaries of a given range of coupling coefficient do not correspond to the same PTE. The minimum PTE is observed at $k = k_{min}$ and the maximum PTE is observed at $k = k_{max}$:

$$\eta_{min} = \eta(k_{min}) = \eta(k_{crit}) \frac{2}{\alpha^2 + 1} \quad (21)$$

$$\eta_{max} = \eta(k_{max}) = \eta(k_{crit}) \frac{2\alpha^2}{\alpha^2 + 1} \quad (22)$$

An increase in α leads to a wider range of possible values of PTE that can be observed in a given range of coupling coefficient.

B. IPT SYSTEM WITH MAXIMIZED PTE

PTE of an IPT system is proportional to the ratio of coupling coefficient to the critical coupling. To achieve high PTE, the system must be designed to have this ratio as high as possible. In the following analysis only IPT systems with PTE greater than 50% are considered. This condition can be formulated as:

$$k_{max} > k_{min} \geq k_{crit} \quad (23)$$

MT of an IPT system operating above the critical coupling in a given range of the coils misalignment $k_{min} \dots k_{max}$ can be defined as:

$$MT = \frac{P_L(k_{max})}{P_L(k_{min})} \quad (24)$$

The following expression for MT can be derived by substituting (11) into (24):

$$MT = \frac{k_{max}^2}{k_{min}^2} \left(\frac{k_{min}^2 + k_{crit}^2}{k_{max}^2 + k_{crit}^2} \right)^2 \quad (25)$$

In general case, MT of an IPT system operating above the critical coupling cannot be reduced to a function of α only, as opposed to MT of an IPT system operating in the vicinity of the critical coupling. The value of the critical coupling and, hence, electrical circuit parameters of the system must be taken into account in addition α to estimate MT in such system. However, two distinguishable boundary cases can be considered for further evaluation of the performance of an IPT system operating above the critical coupling. In its turn, these boundary cases can once again be represented as a function of the single parameter α as will be shown later.

First case corresponds to the IPT system operating just above the critical coupling. Formally, this means that the lowest coupling coefficient in the given range of the coils misalignment coincides with the critical coupling, i.e. $k_{min} = k_{crit}$.

Second case corresponds to the IPT system having very high ratio of the coupling coefficient to the critical coupling. Formally, this means that the lowest coupling coefficient is much greater than the critical coupling $k_{min} \gg k_{crit}$.

For $k_{min}=k_{crit}$ (25) can be represented as:

$$MT = \frac{k_{max}^2}{k_{min}^2} \left(\frac{2k_{min}^2}{k_{max}^2 + k_{min}^2} \right)^2 = \frac{4\alpha^4}{(\alpha^2 + 1)^2} \quad (26)$$

For $k_{min} \gg k_{crit}$ (25) can be represented as:

$$MT = \frac{k_{min}^2}{k_{max}^2} = \alpha^{-4} \quad (27)$$

Thus, the boundaries of MT in an IPT system operating above the critical coupling are functions of the single parameter α and, therefore, geometrical parameters of the

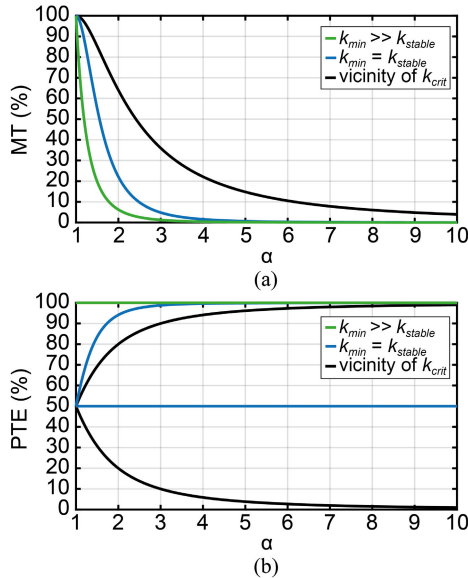


FIGURE 7. MT (a) and PTE (b) as a function of α for different IPT systems: - IPT system operating in the vicinity of the critical coupling - IPT system operating above the critical coupling for $k_{min} = k_{crit}$ - IPT system operating above the critical coupling for $k_{min} \gg k_{crit}$.

coils. Fig. 7a depicts how minimum and maximum achievable MT change with α in an IPT system operating above the critical coupling. The exact MT for a given IPT system lies between the two boundary values and is affected by the value of the critical coupling. For the reference, Fig. 7a compares identified boundary cases with MT of an IPT system operating in the vicinity of the critical coupling. It can be seen, that the latter system have significantly higher MT than the former. For example, when $\alpha = 2$, i.e. $k_{max} = 4k_{min}$, in an IPT system operating above the critical coupling MT lies in the range from 6% to 22%. At the same time, MT equals to 64% in an IPT system operating in the vicinity of the critical coupling.

In a similar manner, PTE of an IPT system operating above the critical coupling can be found. Both the minimum and maximum PTE are evaluated that are observed at $k = k_{min}$ and $k = k_{max}$, correspondingly. For the case of $k_{min} = k_{crit}$, PTE can be calculated as follows:

$$\eta_{min} = \eta(k_{crit}) \tag{28}$$

$$\eta_{max} = \eta(k_{crit}) \frac{2(k_{max}/k_{min})^2}{1 + (k_{max}/k_{min})^2} = \eta(k_{crit}) \frac{2\alpha^4}{\alpha^4 + 1} \tag{29}$$

For the case of $k_{min} \gg k_{crit}$, both the minimum and maximum PTE tend to 100% and can be found as follows:

$$\eta_{min} \cong 2\eta(k_{crit}) \tag{30}$$

$$\eta_{max} \cong 2\eta(k_{crit}) \tag{31}$$

Fig. 7b depicts the range of possible PTE that can be achieved for a given value of α in the IPT system operating above the critical coupling. For the reference, PTE of an IPT system operating in the vicinity of the critical coupling are also shown in Fig. 7b. An IPT system operating above

the critical coupling has improved PTE characteristics in comparison to an IPT system operating in the vicinity of critical coupling. For example, when $\alpha = 2$, i.e. $k_{max} = 4k_{min}$ in an IPT system operating above the critical coupling for $k_{min} \gg k_{crit}$ PTE tends to 100%, while for $k_{min} = k_{crit}$ it can vary from 50% to 95%. The exact value of PTE is defined by the proximity of the system to the critical coupling. PTE of an IPT system operating in the vicinity of the critical coupling can vary from 20% to 80%.

An IPT system operating in the vicinity of the critical coupling have higher MT than an IPT system operating above the critical coupling. However, disadvantage of the former system is lower PTE than that of the latter. Moreover, PTE of the former system can vary significantly during its operation. Therefore, there is no predefined answer to which of the two systems is better. The use of complex performance metrics can aid the choice between the two systems, as well as their further optimization.

IV. OPTIMIZATION OF THE COILS AND IPT SYSTEM DESIGN CONSIDERATIONS

The primary purpose of this Section is to demonstrate the application of the formulated design principles in a clear way by demonstrating straightforward optimization procedures. PDL, PTE and MT can be represented as functions of α , that, in its turn, is solely a function of the coils geometry. This allows for the development of formal methods for the optimization of coils geometrical parameters in order to regulate the performance metrics of an IPT system. We provide two examples of such procedures to illustrate this idea: coils optimization algorithm for maximizing MT, and algorithm for maximizing MT with given coils.

Now, that definitive performance metric for maximizing MT is introduced, an exemplary optimization procedures can be build around it. The goal of the procedure is maximization of MT of the IPT system through minimization of α . Coupling coefficient is a function of coils geometry and mutual position of the coils. Therefore, the optimization procedure can be modified for different parameterized variables. In our example, we use two variables is number of turns in the transmitter and receiver, however similar procedures can be designed to optimize other parameters of the coil, e.g. the inner radii and pitch of the coil, or coils with different shapes, e.g. DD coils or helix coils. Fig. 8 demonstrates an exemplary direct double-variable optimization procedure for the single-layer coils. Design variables are number of turns in transmitting and receiving coils. All the remaining parameters, i.e. outer radii of the coils, coils wire cross-section radius and coils pitch, are fixed. The coils optimization procedure starts with the coils with single turn in both transmitting and receiving coils. For this initial geometry the buffer value of α which we named α_0 is calculated. After that the number of turns is changed throughout the procedure and α is calculated for the changed geometry. If α is lower than α_0 then current α is assigned to the buffer α_0 , the number of turns is increased,

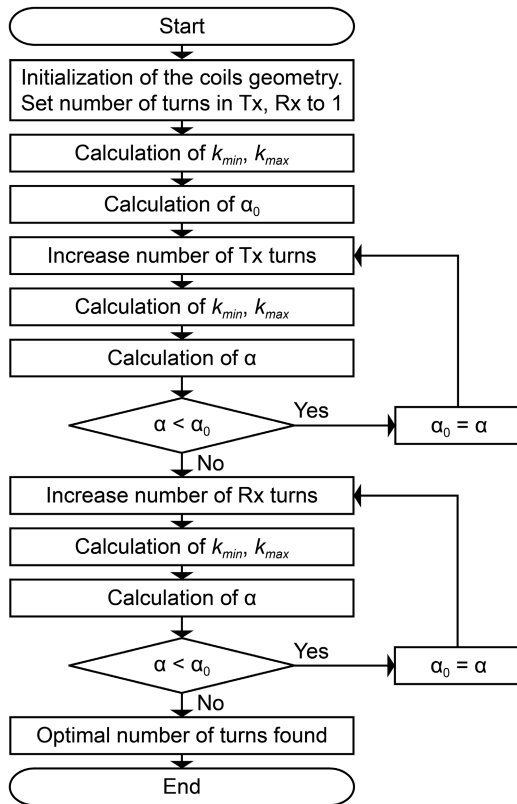


FIGURE 8. Exemplary coils geometry optimization procedure. The goal of the procedure is to maximize MT via minimization of α . At the start both coils have only one turn of wire. All the remaining geometrical parameters, including outer radii of the coils, are constant. With each iteration the number of turns in the coils is increased, if it leads to lower α .

and the process repeats. The procedure continues until the increase in number of turns in the coils leads to decrease in α .

Design space for two different radii of the transmitting coil 30 mm and 42 mm, as well as three different ranges of the axial distance, i.e. $5 \cdot \cdot 15$ mm, $15 \cdot \cdot 25$ mm and $5 \cdot \cdot 25$ mm are depicted in Fig. 9. Receiving coil radius was set as 30 mm. Coils wire cross-section radius was set as 0.25 mm, coils pitch was 2 mm. The number of turns ranges from a single turn to a number corresponding to a completely filled coil. From Fig. 9, it becomes clear that asymmetrical number of turns in transmitting and receiving coils leads to an IPT system with a minimum α . Thus, one of the coils should be designed to have a low number of turns in order to maximize MT. If both coils are completely filled with the wire, the IPT system will have high α and low MT.

It is an important result that α can be changed significantly via coils geometry optimization even for a fixed outer radii of coils. This once again stresses the importance of the coils geometry optimization. Coils with arbitrary defined geometry can deteriorate the performance of an IPT system. In its turn, more complex optimization procedures of the coils (e.g. procedures based on heuristic algorithms) than the one described in this paper, with more indulgent constraints on the geometry of the coils and with α as the objective function can

lead to even higher MT. Development of such optimization procedures can be a direction for a future work.

The second exemplary optimization procedure considers maximizing MT for the set coils, for example, ‘off the shelf’ coils (Fig. 10). After coils design is set, an IPT system can be built around the coil couple. The IPT system with maximized PDL is optimized. Input design parameters are geometry of the coils, their resulting self-inductances L_T , L_R and coupling coefficient range boundaries k_{min} , k_{max} . The design procedure starts with the calculation of the stable critical coupling k_{stable} using (15). The product of C_T and C_R can be calculated using (3), (4) and (10):

$$C_T C_R = \frac{k_{stable}^4 L_T L_R}{R_T^2 (R_R + R_L)^2} \quad (32)$$

The exact value of C_T and C_R of the IPT system can be found by substituting (32) into (1):

$$C_T = \frac{k_{stable}^2 L_R}{R_T (R_R + R_L)} \quad (33)$$

$$C_R = \frac{k_{stable}^2 L_T}{R_T (R_R + R_L)} \quad (34)$$

In order to estimate C_T and C_R , an educated guess must be made on the resonant frequency of the system, because the value of the capacitors is a function R_T and R_R , which, in turn, depend on the operating frequency of the system. After C_T and C_R are estimated, the resonant frequency of the IPT system can be calculated using (1) for the known inductances and capacitances in the circuit. After the first iteration of the design is complete, R_T and R_R and, subsequently, C_T and C_R need to be recalculated for the newly estimated operating frequency of the system. This recalculation is repeated until the resonant frequency of the system is properly defined.

V. EXPERIMENTAL VERIFICATION

Experimental measurements were conducted to verify the presented results. The measurement setup (Fig. 11a) consisted of a waveform generator, transmitting and receiving parts of an IPT system, a coils-positioning device and a measurement equipment. The function generator Tektronix AFG3252 was used to drive the transmitting part of the IPT system with sinusoidal waveform. Equivalent electrical circuit of the setup is shown in Fig. 11b. The generator was a current source with source resistance R_S in parallel. Shunt resistor R_{shunt} was placed at the output of the signal generator to reduce the large 50Ω resistance of the waveform generator. Using Thevenin’s theorem, the transmitting part of the measurement setup can be represented as voltage source V_{Seq} with series resistance R_{Seq} . The values of R_{Seq} and V_{Seq} can be calculated as:

$$R_{Seq} = \frac{R_S R_{shunt}}{R_S + R_{shunt}} \quad (35)$$

$$V_{Seq} = I_S R_{Seq} \quad (36)$$

Total resistance of the transmitting part of the IPT system consisted of the equivalent source resistance R_{Seq} and the

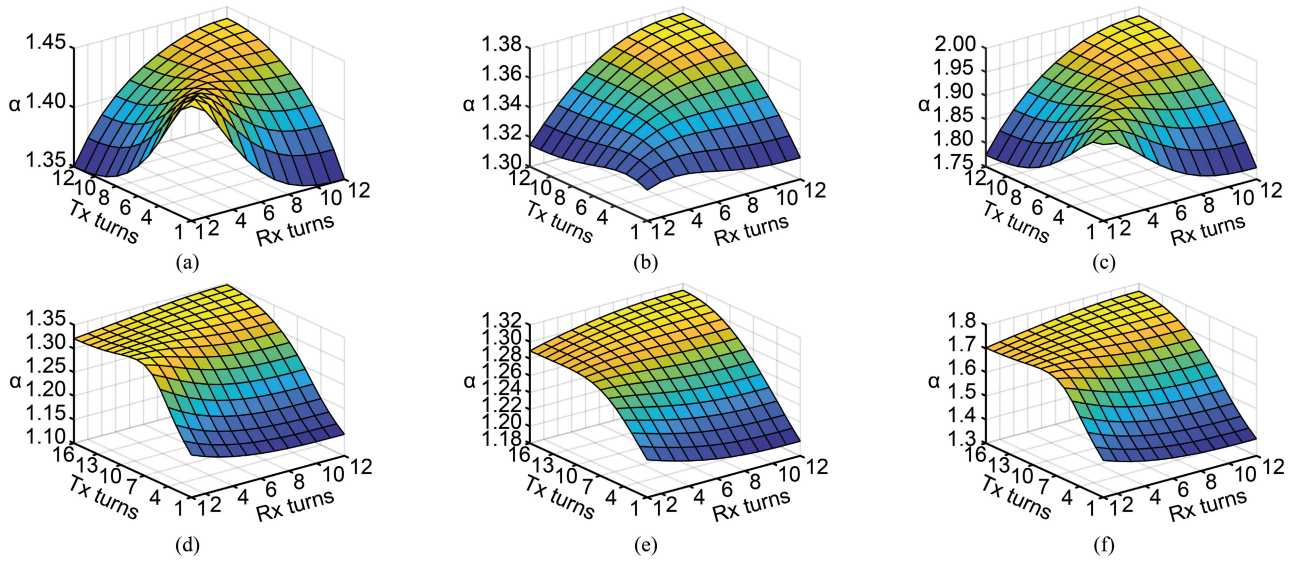


FIGURE 9. Parameter α as a function of number of turns in the transmitting and receiving coils of an IPT system for the transmitting coil with outer radii 30 mm (a, b, c) and for the transmitting coil with outer radii 42 mm (d, e, f). The axial distance between the coils is 5... 15 mm (a, d), 15... 25 mm (b, e), 5... 25 mm (c, f). Lower α corresponds to the better tolerance to the coils misalignments in the IPT system.

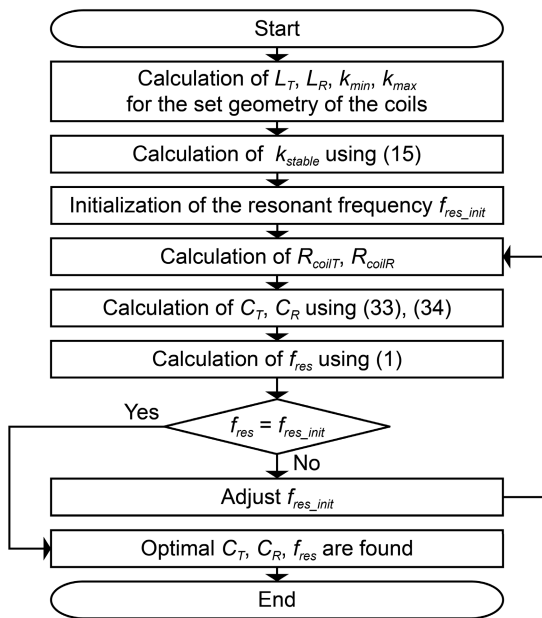


FIGURE 10. Exemplary optimization procedure for the IPT system with set coils geometry. The considered system is built for PDL maximization. Therefore, k_{stable} is evaluated for the given boundaries of the coils misalignment range k_{min} and k_{max} . For the calculated k_{stable} , C_T and C_R can be found. The resonant frequency of the system is calculated afterwards. The procedure is iterative, because R_T and R_R are functions of frequency, and the frequency cannot be known beforehand.

equivalent series resistance of the transmitting coil R_{coilT} :

$$R_T = R_{S_{eq}} + R_{coilT} \quad (37)$$

In addition to the shunt resistor transmitting part PCB included compensating capacitance C_T . Receiving part PCB included load resistor R_L and compensating capacitance C_R .

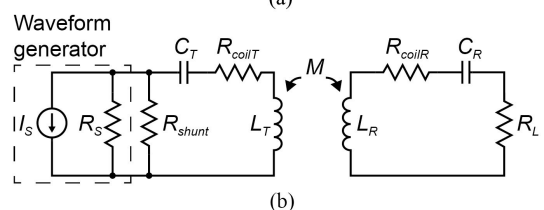
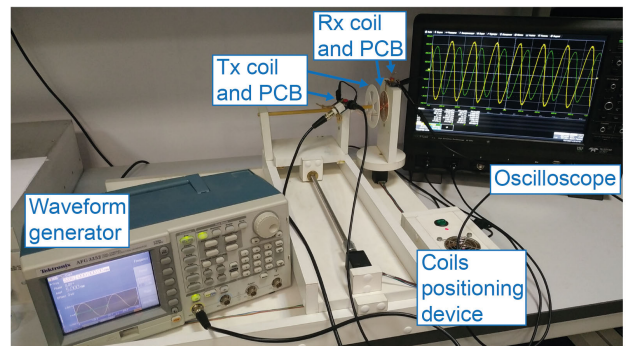


FIGURE 11. Photograph of the measurement setup consisting of a waveform generator, transmitting and receiving parts of the IPT system, coils-positioning device and measurement equipment (a) and its electrical circuit (b).

The experiment was divided into two parts:

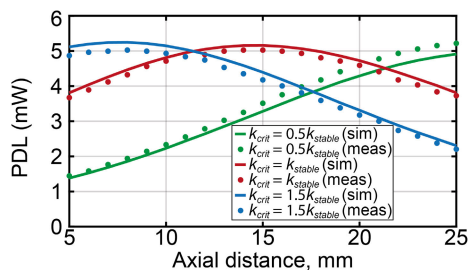
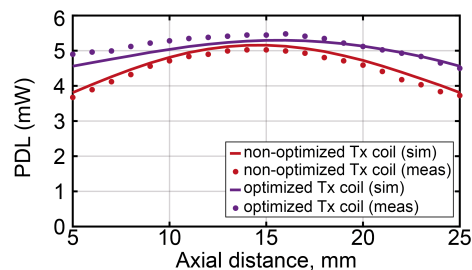
- 1) an illustration of the concept of the optimal value of the critical coupling for a given range of the coils misalignments.
- 2) a comparison of IPT systems with optimized and non-optimized coils.

A. OPTIMAL VALUE OF THE CRITICAL COUPLING

The goal of this study was an experimental validation of (15) for calculation of the optimal critical coupling that

TABLE 2. Parameters of the IPT systems with different critical coupling: $k_{crit} = 0.5k_{stable}$, $k_{crit} = k_{stable}$, $k_{crit} = 1.5k_{stable}$, and non-optimized and optimized geometry of the transmitting coil.

	System no.1		System no.2		System no.3		System no.4	
	$k_{crit} = k_{stable}$		$k_{crit} = 0.5k_{stable}$		$k_{crit} = 1.5k_{stable}$		$k_{crit} = k_{stable}$	
	Simulated	Measured	Simulated	Measured	Simulated	Measured	Simulated	Measured
Inductance L_T (μH)	8.97	8.98	8.97	8.98	8.97	8.98	2.38	2.43
Transmitting coil ESR R_{coilT} ($\text{m}\Omega$)	391	420	535	512	326	344	284	282
Capacitance C_T (nF)	4.19	4.18	1.01	1.00	9.60	9.70	1.76	1.64
Inductance L_R (μH)	3.42	3.42	3.42	3.42	3.42	3.42	3.42	3.42
Receiving coil ESR R_{coilR} ($\text{m}\Omega$)	230	248	315	325	191	202	365	410
Capacitance C_R (nF)	11.00	11.00	2.66	2.67	25.18	24.60	1.23	1.12
Operating frequency f (kHz)	821		1668		542		2458	

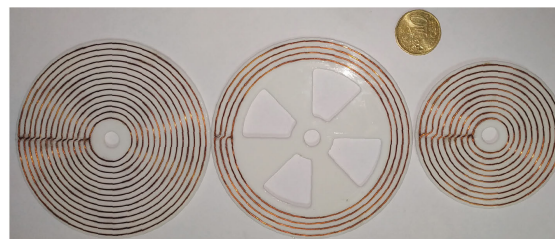
**FIGURE 12.** PDL of IPT systems with different critical coupling, i.e. $k_{crit} = 0.5k_{stable}$, $k_{crit} = k_{stable}$, $k_{crit} = 1.5k_{stable}$, as a function of the axial distance between the coils. Parameters of the systems are given in Table 2.**FIGURE 13.** PDL of IPT systems operating in the vicinity of the critical coupling with non-optimized and optimized coils. Parameters of the systems are given in Table 2.

corresponds to the highest MT in an IPT system operating in the vicinity of the critical coupling.

Three IPT systems operating in the vicinity of critical coupling were compared. The parameters of these systems are given in Table 2. System no.1 was tuned to operate at the value of critical coupling equal to k_{stable} , System no.2 was tuned to $0.5k_{stable}$, and System no.3 was tuned to $1.5k_{stable}$. The systems were designed following the considerations given in Section IV. Geometry of the coils was identical for all three systems. Transmitting and receiving coil outer radii were set as 42 mm and 30 mm, corresponding number of turns was 14 and 10. Wire radius and coils pitch were equal in both coils and set as 0.25 mm and 2 mm. Resulting self-inductance of the transmitting and receiving coils were $8.97 \mu\text{H}$ and $3.42 \mu\text{H}$. Parameters of the source $V_{Seq} = 320 \text{ mV}$, $R_{Seq} = 4.55 \Omega$ and the load resistance $R_L = 20 \Omega$ were identical also.

Changes in coupling coefficient were caused by changes in the distance between the coils from 5 to 25 mm. For the given coils in the given range of the misalignments α is equal to 1.76. Fig. 12 depicts PDL of the IPT systems as a function of the axial distance.

Measured MT of System no.1 is equal to 73%. Measured MT of System no.2 and System no.3 have lower MT, i.e. 28% and 44%. For the exemplary IPT prototype PTE is about 50% for the fully aligned coils. Misalignment of the coils leads to the changes in the efficiency from 30% to 70%.

**FIGURE 14.** The coils used in the experiment (from left to right): transmitting coil with non-optimized geometry, optimized geometry and receiving coil.

B. OPTIMIZATION OF THE COILS

The goal of this study was an experimental verification of the efficacy of the procedure for optimization of coils geometry described in Section V. System no.1 in Table 2 represents the system with initial, or non-optimized, coil couple geometry. Axial distance between the coils changed in the range from 5 to 25 mm. The resulting α calculated for this configuration is equal to 1.76. In order to minimize α , the coils geometry optimization procedure was conducted. Receiving coil parameters have not changed as a result of the optimization. At the same time number of turns in the transmitting coil has decreased from 14 to 4. The self-inductance of the optimized transmitting coil was equal to $2.38 \mu\text{H}$. The optimization lead to 19% reduction in α , down to 1.48. The transmitting coil with even fewer number of turns would have led to even lower α . However, as we can see from Fig. 8f the change in α would have been negligible.

At the same time this would have led to lower self-inductance of the coil and higher operating frequency of the system. The System no.4 in Table 2 was build around the optimized coil couple. This system operates in the vicinity of the critical coupling.

PDL as a function of the axial distance is depicted in Fig. 13 for the systems with optimized and non-optimized coils. The measured MT of System no.1 that uses non-optimized coils is equal to 73%, while the measured MT of System no.4 that uses optimized coils is equal to 82% (86% simulated). The resulting geometry of the coils is depicted in Fig. 14.

VI. CONCLUSION

In this paper we have outlined the basis for several design principles for IPT systems with maximum possible inherent tolerance to misalignment of the coils. These principles can be summarized as follows:

1. The relative change in PDL and PTE caused by the coils misalignment is affected by two parameters: a relation of the coupling coefficient and the critical coupling, and also by a relation of the maximum to minimum coupling coefficient in a given range of the coils misalignment (parameter α). Corresponding characteristic curves are similar for IPT systems with different operating frequencies, load resistance, etc. Thus, it is possible to generalize the presented design methodology for any IPT systems with SS-compensation including those built around class D power amplifier.

2. To achieve the theoretical limit of misalignment tolerance for a given coil couple and preset values of expected (possible) misalignment one must tuned IPT systems in such a manner that critical coupling coefficient could be equal to the square root of product of maximum coupling coefficient by minimum coupling coefficient. It is of special importance for design of IPT systems with prefabricated (commercial) coil set. Additionally, the stable coupling coefficient (k_{stable}) can be used to inform the choice between PDL and PTE as described below.

3. To evaluate the IPT misalignment tolerance we introduced two new metrics. The first one, which we refer to as misalignment tolerance (MT), is defined as the ratio of minimum to maximum PDL in a given range of the coils misalignment. MT is a function of magnetic properties of the coil couple only. Therefore, the main factor limiting tolerance of an IPT system to the coils misalignment is properly optimized geometry of the coils. Consequently, informed proper optimization of the coils is of crucial importance for designing an IPT system with high misalignment tolerance. All other means should be used only in combination with and after the proper design of coils.

4. The second new metric proposed in this paper is α , the square root from the ratio of maximum to minimum coupling coefficient. This metric is necessary to inform and direct the coil geometry optimization targeting the tolerance to the coils misalignment. The general principle here is that to improve the MT one must change the coil geometry in such a way that α becomes as close to 1 as possible taking another limitations

into account (coil heating, for example). More specifically, we have shown that the α is lower for the asymmetric coils, with significantly different number of turns.

5. To inform the unavoidable choice between MT, PTE and PDL the stable coupling coefficient (k_{stable}) can be used as a yardstick. If IPT system is tuned in such a way that $k_{min} \leq k_{crit} \leq k_{stable}$ than the maximum possible PDL can be achieved and PTE would be higher than 50% for most part of the given misalignment range. In this case the closer the k_{crit} to the k_{stable} the higher the MT and the closer k_{crit} to the k_{min} the higher the PTE. It should be stressed that the tuning in which $k_{stable} \leq k_{crit} \leq k_{max}$ did not have any significant advantage and must be avoided.

The application of these principles to high-frequency IPT systems will require taking into account additional restrictions and design necessities such as required impedance matching.

Finally, we want to emphasize that these principles are not limited to the specific IPT system with SS-compensation that was considered in this paper. They can potentially be applied to different IPT systems, including those utilizing feedback loops and control circuitry, to increase the tolerance to the coils misalignment. By incorporating these design principles the inherent tolerance to the misalignment will be increased, and the requirements to the control circuitry will be reduced, therefore, leading to the better overall performance of the system.

REFERENCES

- [1] G. A. Covic and J. T. Boys, "Inductive power transfer," *Proc. IEEE*, vol. 101, no. 6, pp. 1276–1289, Jun. 2013, doi: [10.1109/JPROC.2013.2244536](https://doi.org/10.1109/JPROC.2013.2244536).
- [2] G. L. Barbruni, P. M. Ros, D. Demarchi, S. Carrara, and D. Ghezzi, "Miniaturised wireless power transfer systems for neurostimulation: A review," *IEEE Trans. Biomed. Circuits Syst.*, vol. 14, no. 6, pp. 1160–1178, Dec. 2020, doi: [10.1109/TBCAS.2020.3038599](https://doi.org/10.1109/TBCAS.2020.3038599).
- [3] A. Mahesh, B. Chokkalingam, and L. Mihet-Popa, "Inductive wireless power transfer charging for electric vehicles—A review," *IEEE Access*, vol. 9, pp. 137667–137713, 2021, doi: [10.1109/ACCESS.2021.3116678](https://doi.org/10.1109/ACCESS.2021.3116678).
- [4] B. Luo, T. Long, L. Guo, R. Dai, R. Mai, and Z. He, "Analysis and design of inductive and capacitive hybrid wireless power transfer system for railway application," *IEEE Trans. Ind. Appl.*, vol. 56, no. 3, pp. 3034–3042, May 2020, doi: [10.1109/TIA.2020.2979110](https://doi.org/10.1109/TIA.2020.2979110).
- [5] C. R. Teeneti, T. T. Truscott, D. N. Beal, and Z. Pantic, "Review of wireless charging systems for autonomous underwater vehicles," *IEEE J. Ocean. Eng.*, vol. 46, no. 1, pp. 68–87, Jan. 2021, doi: [10.1109/JOE.2019.2953015](https://doi.org/10.1109/JOE.2019.2953015).
- [6] L. Xie, J. Xu, and R. Zhang, "Throughput maximization for UAV-enabled wireless powered communication networks," *IEEE Internet Things J.*, vol. 6, no. 2, pp. 1690–1703, Apr. 2019, doi: [10.1109/JIOT.2018.2875446](https://doi.org/10.1109/JIOT.2018.2875446).
- [7] S. Jayalath and A. Khan, "Design, challenges, and trends of inductive power transfer couplers for electric vehicles: A review," *IEEE J. Emerg. Sel. Topics Power Electron.*, vol. 9, no. 5, pp. 6196–6218, Oct. 2021, doi: [10.1109/JESTPE.2020.3042625](https://doi.org/10.1109/JESTPE.2020.3042625).
- [8] M. Haerinia and R. Shadid, "Wireless power transfer approaches for medical implants: A review," *Signals*, vol. 1, no. 2, pp. 209–229, Dec. 2020, doi: [10.3390/signals1020012](https://doi.org/10.3390/signals1020012).
- [9] A. M. Jawad, R. Nordin, S. K. Gharghan, H. M. Jawad, and M. Ismail, "Opportunities and challenges for near-field wireless power transfer: A review," *Energies*, vol. 10, no. 7, p. 1022, Jul. 2017, doi: [10.3390/en10071022](https://doi.org/10.3390/en10071022).

- [10] E. Okamoto, Y. Yamamoto, Y. Akasaka, T. Motomura, Y. Mitamura, and Y. Nosé, "A new transcutaneous energy transmission system with hybrid energy coils for driving an implantable biventricular assist device," *Artif. Organs*, vol. 33, no. 8, pp. 622–626, Aug. 2009, doi: [10.1111/j.1525-1594.2009.00785.x](https://doi.org/10.1111/j.1525-1594.2009.00785.x).
- [11] B. S. Wilson, "Cochlear implants: Current designs and future possibilities," *J. Rehabil. Res. Develop.*, vol. 45, no. 5, pp. 695–730, Dec. 2008, doi: [10.1682/jrrd.2007.10.0173](https://doi.org/10.1682/jrrd.2007.10.0173).
- [12] W. Xiong, Q. Yu, Z. Liu, Q. Zhu, M. Su, L. Zhao, and A. P. Hu, "A dual-frequency-detuning method for improving the coupling tolerance of wireless power transfer," *IEEE Trans. Power Electron.*, vol. 38, no. 6, pp. 6923–6928, Jun. 2023, doi: [10.1109/TPEL.2023.3253904](https://doi.org/10.1109/TPEL.2023.3253904).
- [13] J.-J. Kao, C.-L. Lin, Y.-C. Liu, C.-C. Huang, and H.-S. Jian, "Adaptive bidirectional inductive power and data transmission system," *IEEE Trans. Power Electron.*, vol. 36, no. 7, pp. 7550–7563, Jul. 2021, doi: [10.1109/TPEL.2020.3047069](https://doi.org/10.1109/TPEL.2020.3047069).
- [14] Y. Zhang, W. Pan, H. Wang, Z. Shen, Y. Wu, J. Dong, and X. Mao, "Misalignment-tolerant dual-transmitter electric vehicle wireless charging system with reconfigurable topologies," *IEEE Trans. Power Electron.*, vol. 37, no. 8, pp. 8816–8819, Aug. 2022, doi: [10.1109/TPEL.2022.3160868](https://doi.org/10.1109/TPEL.2022.3160868).
- [15] L. Zhao, D. J. Thrimawithana, U. K. Madawala, A. P. Hu, and C. C. Mi, "A misalignment-tolerant series-hybrid wireless EV charging system with integrated magnetics," *IEEE Trans. Power Electron.*, vol. 34, no. 2, pp. 1276–1285, Feb. 2019, doi: [10.1109/TPEL.2018.2828841](https://doi.org/10.1109/TPEL.2018.2828841).
- [16] M. Kim, D.-M. Joo, and B. K. Lee, "Design and control of inductive power transfer system for electric vehicles considering wide variation of output voltage and coupling coefficient," *IEEE Trans. Power Electron.*, vol. 34, no. 2, pp. 1197–1208, Feb. 2019, doi: [10.1109/TPEL.2018.2835161](https://doi.org/10.1109/TPEL.2018.2835161).
- [17] Y. Chen, R. Mai, Y. Zhang, M. Li, and Z. He, "Improving misalignment tolerance for IPT system using a third-coil," *IEEE Trans. Power Electron.*, vol. 34, no. 4, pp. 3009–3013, Apr. 2019, doi: [10.1109/TPEL.2018.2867919](https://doi.org/10.1109/TPEL.2018.2867919).
- [18] J. Feng, Q. Li, F. C. Lee, and M. Fu, "Transmitter coils design for free-positioning omnidirectional wireless power transfer system," *IEEE Trans. Ind. Informat.*, vol. 15, no. 8, pp. 4656–4664, Aug. 2019, doi: [10.1109/TII.2019.2908217](https://doi.org/10.1109/TII.2019.2908217).
- [19] Y. Li, J. Zhao, Q. Yang, L. Liu, J. Ma, and X. Zhang, "A novel coil with high misalignment tolerance for wireless power transfer," *IEEE Trans. Magn.*, vol. 55, no. 6, pp. 1–4, Jun. 2019, doi: [10.1109/TMAG.2019.2904086](https://doi.org/10.1109/TMAG.2019.2904086).
- [20] A. A. Danilov, R. R. Aubakirov, E. A. Mindubaev, K. O. Gurov, D. V. Telyshev, and S. V. Selishchev, "An algorithm for the computer aided design of coil couple for a misalignment tolerant biomedical inductive powering unit," *IEEE Access*, vol. 7, pp. 70755–70769, 2019, doi: [10.1109/ACCESS.2019.2919259](https://doi.org/10.1109/ACCESS.2019.2919259).
- [21] Z. Zhang and B. Zhang, "Angular-misalignment insensitive omnidirectional wireless power transfer," *IEEE Trans. Ind. Electron.*, vol. 67, no. 4, pp. 2755–2764, Apr. 2020, doi: [10.1109/TIE.2019.2908604](https://doi.org/10.1109/TIE.2019.2908604).
- [22] F. Liu, Y. Yang, D. Jiang, X. Ruan, and X. Chen, "Modeling and optimization of magnetically coupled resonant wireless power transfer system with varying spatial scales," *IEEE Trans. Power Electron.*, vol. 32, no. 4, pp. 3240–3250, Apr. 2017, doi: [10.1109/TPEL.2016.2581840](https://doi.org/10.1109/TPEL.2016.2581840).
- [23] J. Al Sinayyid, H. Takhedmit, P. Poulichet, M. Grzeskowiak, A. Diet, and G. Lissorgues, "A reconfigurable coil grid for receiver localization in wireless power transfer and magnetic field steering," *IEEE J. Radio Freq. Identificat.*, vol. 5, no. 2, pp. 128–138, Jun. 2021, doi: [10.1109/JRFID.2020.3046677](https://doi.org/10.1109/JRFID.2020.3046677).
- [24] M. Grzeskowiak, A. Diet, M. Benamara, P. Poulichet, C. Conessa, S. Protat, M. Biancheri-Astier, F. de Oliveira Alves, Y. Le Bihan, and G. Lissorgues, "Distributed diameter subcoil twisted loop antenna in nonradiative WPT," *IEEE Antennas Wireless Propag. Lett.*, vol. 17, no. 1, pp. 4–7, Jan. 2018, doi: [10.1109/LAWP.2017.2767020](https://doi.org/10.1109/LAWP.2017.2767020).
- [25] M. Kiani and M. Ghovanloo, "A figure-of-merit for design of high performance inductive power transmission links for implantable microelectronic devices," in *Proc. Annu. Int. Conf. IEEE Eng. Med. Biol. Soc.*, San Diego, CA, USA, Aug. 2012, pp. 847–850, doi: [10.1109/EMBC.2012.6346064](https://doi.org/10.1109/EMBC.2012.6346064).
- [26] N. D. N. Donaldson and T. A. Perkins, "Analysis of resonant coupled coils in the design of radio frequency transcutaneous links," *Med. Biol. Eng. Comput.*, vol. 21, no. 5, pp. 612–627, Sep. 1983, doi: [10.1007/BF02442388](https://doi.org/10.1007/BF02442388).



EDUARD MINDUBAEV (Member, IEEE) received the B.S., M.S., and Ph.D. degrees in electronic engineering from the National Research University of Electronic Technology, Moscow, Russia, in 2011, 2013, and 2018, respectively.

He is currently a Senior Engineer with the Laboratory of Wireless Biomedical Interfaces, Institute of Biomedical Systems, National Research University of Electronic Technology. He has authored and coauthored about 40 technical articles. His current research interests include wireless energy transfer, specifically its application to implantable medical devices.



KONSTANTIN GUROV (Member, IEEE) received the B.S. and M.S. degrees in electronic engineering from the National Research University of Electronic Technology, Moscow, Russia, in 2016 and 2018, respectively, where he is currently pursuing the Ph.D. degree. Currently, he is an Assistant Professor with the Institute of Biomedical Systems, National Research University of Electronic Technology. He has authored and coauthored about 30 technical articles. His current research interests include implantable medical device development and electrical and electronics engineering research and design.



SERGEY SELISHCHEV (Senior Member, IEEE) received the Dipl.-Ing. degree from the National Research University of Electronic Engineering, Moscow, Russia, in 1976, the Ph.D. degree in physics and mathematics from the Institute of Metallurgy and Material Sciences, Russian Academy of Sciences, in 1983, and the Dr.-Sc. degree in physics and mathematics from the Institute of Thermophysics, Russian Academy of Sciences, in 1988.

In 1993, he initiated the teaching of biotechnical and medical devices and systems with the National Research University of Electronic Technology. In 1999, he founded the Department of Biomedical Systems, Institute of Biomedical Systems, since 2018, at this institution and chaired it since foundation. He was a Project Leader in the development of the first Russian automated defibrillator and the first Russian ventricular assist device, namely, Sputnik. He is currently the Director of the Institute of Biomedical Systems, National Research University of Electronic Technology. He has authored and coauthored more than 200 scientific and technical articles. He is the Editor-in-Chief of the Russian journal *Meditsynskaya Tekhnika*, which is translated and published in English under the title *Biomedical Engineering*.



ARSENY DANILOV (Member, IEEE) received the B.S. and M.S. degrees in electronic engineering and the Ph.D. degree in physics and mathematics from the National Research University of Electronic Technology, Moscow, Russia, in 2002, 2004, and 2007, respectively.

He is currently the Head of the Laboratory of Wireless Biomedical Interfaces, Institute of Biomedical Systems, National Research University of Electronic Technology. He has authored and coauthored about 50 articles. His current research interests include the design of implantable medical devices and the investigation of the interaction between biological tissues and electromagnetic fields and waves. He is the Deputy Editor-In-Chief of the Russian journal *Meditsynskaya Tekhnika*, which is translated and published in English under the title *Biomedical Engineering*.